

Improving the efficiency of frequency domain equalization in conventional coherent optical OFDM system using discrete wavelet transform

AHMET GÜNER^{a,*}, ALİ ÖZEN^b

^a*Bingöl University, Department of Electrical and Electronics Engineering, 12000 Bingöl, Turkey*

^b*Nuh Naci Yazgan University – HARGEM, Department of Electrical and Electronics Engineering, 38010 Kayseri, Turkey*

In this paper, a novel discrete wavelet transform-based coherent optical OFDM system, which improved the performance of the frequency domain equalizer by using discrete wavelet transform in the conventional coherent optical OFDM system, is proposed as a solution to data transmission speed and distance problems limited by the fiber nonlinearity and optical noise of optical channels. The greatest novelty of this study is that the discrete wavelet transforms and coherent optical OFDM systems are combined in the proposed technique. Simulation results are shown to verify the effectiveness of the proposed system at high launch power levels where fiber nonlinearity is significant.

(Received December 5, 2018; accepted October 9, 2019)

Keywords: Coherent optical-OFDM systems, Discrete wavelet transform, Fiber nonlinearity impairment, Frequency domain equalizer, Radio over Fiber

1. Introduction

As a result of today's increasing demands, data communication capacity and the speed of communication systems is of significant importance. For this reason, new communication technologies are constantly needed, and some of the more prominent are Radio-over-Fiber (RoF) systems. RoF systems are a powerful solution that broadens capacity and mobility by combining wireless and optical systems [1]. RoF systems are easily combined with the coherent optical-OFDM (CO-OFDM) system, which is recommended as the future optical communication method as it supports high data rates and efficient bandwidths for long-haul transmission systems.

Optical systems enable the use of new digital processing techniques in the receiver for faster data transmission over long-distances. For example, high spectral efficiency is achieved by using OFDM, a multi-carrier multiplex technique [2]. In addition, the data transmission speed can be increased, especially for long-distance transmissions, by high-level digital modulation [3]. However, to benefit from these advantages, especially for RoF systems within optical systems, it is first necessary to determine the optical channel in the receiver and to perform equalization processes to correct the negative effects of the channel.

In an optical communication system, fiber attenuation, dispersion such as polarization-mode dispersion (PMD) and chromatic dispersion (CD), and nonlinearity such as self-phase modulation and cross-phase modulation, combined with optical noise cause adverse effects on system performance. Fiber nonlinear effects deteriorate

system performance and have become the major performance limiting factor of optical communication systems. However, in CO-OFDM systems, equalizers are used in order to reduce fiber nonlinearity and the linear effects of optical channels [4–6].

In this paper, performance analysis was conducted by taking into consideration the fiber nonlinearity effect of the optical channel, which is one of the factors commonly limiting information transmission over long distances in CO-OFDM systems. In particular, fiber nonlinearity causes inter-symbol interference due to the effect of scattering.

When common equalizer schemes are investigated in optical communications systems, they are applied within the frequency domain such as the one-tap frequency domain equalizer [4], the artificial neural network nonlinear equalizer [5], and/or within the time domain such as the Volterra-based equalizer [6], the Decision Feedback Equalizer [7]. In single-carrier optical communication systems, estimation of the channel information and correction of the effects of the impairment in the received signal is performed within the time domain. In CO-OFDM systems, the modulation of the data and the loading to the carrier are performed within the frequency domain. This allows for the estimation and equalization of channel information within the frequency domain.

In many applications, frequency domain channel estimation has been applied to OFDM receivers due to its simplicity. Since one-tap frequency domain equalizers are applied to each OFDM subcarrier, it is easy to implement coherent detection for BPSK, QPSK, and M-QAM.

Scattered-pilots are the typical training signals. On the other hand, lengthy preambles make it possible to carry out

channel estimation within the time domain. By using the time domain long preambles, the impulse responses of the unknown channels can be estimated, and the frequency domain information of the channel obtained by using the FFT. The current study proposes a method of improving estimation accuracy in which channel information within the time domain and channel information within the frequency domain are combined. The study shows that the time domain approach outperformed the frequency domain channel estimation [8].

In this paper, channel estimation and equalization processes were conducted for three different situations, namely frequency-frequency domain (FEFE), time-frequency domain (TEFE), and time-time domain (TETE). In the conventional CO-OFDM system, known channel estimation and equalization methods were compared within time and/or frequency domains. Results showed that frequency domain channel estimation and equalization methods (FEFE) performed poorest [8]. In order to increase the performance of FEFE, which is the simplest to apply, discrete wavelet transform was attempted in the conventional CO-OFDM system.

The Wavelet transform (WT)-based CO-OFDM system was widely studied in [9–11]. However, WT-based CO-OFDM just substitutes the discrete Fourier transform (DFT) and the inverse DFT (IDFT) with the discrete Wavelet transform (DWT) and the inverse DWT (IDWT), respectively. In this paper, a novel discrete wavelet transform-based CO-OFDM system (DWT CO-OFDM-FEFE) is proposed, and which was found to improve the performance of the frequency domain equalizer by using DWT in the conventional CO-OFDM system. Additionally, channel information estimation and equalization process are implemented within the frequency domain. The proposed method combines the CO-OFDM and DWT, thereby improving the performance of the conventional CO-OFDM system. The most significant feature of the proposed method is that the DWT and CO-OFDM systems are combined.

To the best of the author's knowledge no other published works have proposed the same method. This paper investigates the proposed method within the context of time and frequency domain channel equalization in multi carrier communications. When each input data symbol is spread by IDWT before its allocated subcarrier in the transmitter, a signal is obtained with the lower peak to average power ratio (PAPR) in the transmitter, which enhances the efficiency of the frequency domain equalization in the receiver. For this reason, while being computationally close, the proposed DWT CO-OFDM-FEFE system compensates for linear and nonlinear impairment effects more effectively, even at high launch power levels where fiber nonlinearity is significant. In particular, it is extremely satisfactory in achieving an OSNR gain of ~5 dB at the FEC (Forward Error Correction) limit (BER = 10^{-3}) value with the proposed method.

The remainder of this paper is organized as follows: the general structure of the CO-OFDM system, channel

equalization within the frequency domain and channel equalization within the time domain are summarized in Section 2, Section 3, and Section 4, respectively. Transmitter and receiver blocks of the proposed DWT-based CO-OFDM System are explained in detail in Section 5. Computer simulation results and evaluations are given in Section 6 and Section 7.

2. Coherent optical OFDM system

The general structure of the coherent optical OFDM system is shown in Fig. 1. In the transmitter, the datasets are prepared by matching according to the M-QAM modulation type. Then, training symbols are added to the OFDM symbols prior to the inverse FFT (IFFT) process. The RF OFDM signal can be described as in [12]

$$s(t) = \sum_{k=-N_c/2}^{N_c/2-1} a_k e^{jw_k t} \text{ for } 0 \leq t < T_s \quad (1)$$

where a_k is the complex symbol sequence, N_c is the number of subcarriers, w_k is the frequency of the subcarrier and T_s is the OFDM symbol time.

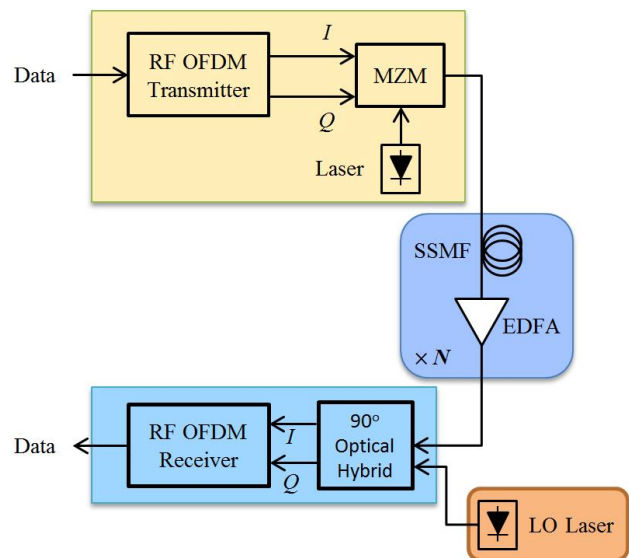


Fig. 1. Block diagram of CO-OFDM system, LO: local oscillator

After the IFFT operation, two optical IQ modulators (Mach-Zehnder Modulator – MZM) are used to convert the electrical signal into an optical signal as

$$E_t(t) = s(t) e^{(jw_{TL}t + \phi_{TL})} \quad (2)$$

where w_{TL} and ϕ_{TL} are the angular frequency and phase of the transmitter laser, respectively. The optical channel includes many standard single mode fiber (SSMF) lengths.

SSMF lengths have impairment effects such as CD, PMD, nonlinear effect and attenuation during signal transmission. In the optical channel, an erbium-doped fiber amplifier (EDFA) is used for attenuations in the transmitted signal over each divided length. The received optical signal after transmission through the optical channel with impulse response $h(t)$ becomes

$$E_r(t) = s(t) e^{(j\omega_{TL}t + \phi_{TL})} * h(t) \quad (3)$$

where $*$ is the convolution product. At the receiver, the optical signal is converted to an electrical signal by a local oscillator laser by passing through a 90° optical hybrid.

$$y(t) = E_r e^{-j\omega_{LO}t + \phi_{LO}} = e^{(j\Delta\omega t + \Delta\phi)} s(t) * h(t) \quad (4)$$

where $\Delta\omega$ is the angular frequency offset, $\Delta\phi$ is the phase offset, ω_{LO} and ϕ_{LO} are the angular frequency and phase of the local oscillator laser. Then, the datasets in the OFDM subcarriers are obtained by the FFT process of the sampled value of Eq. 4.

$$Y_k = H_k a_k + \eta_k \quad (5)$$

where Y_k is the received symbol, H_k is the frequency domain channel response of the k th subcarrier and η_k is the noise. The destructive effects were tried to be removed using the equalizer.

3. Channel equalization in frequency domain

In multicarrier modulations, it is important to estimate high accuracy channel gain for each subcarrier in the receiver. In channel estimation, there are two methods. The first uses the training sequence $y(t)$ within the time domain for channel information before the FFT. The second method uses the Y_k signal after the FFT.

After channel estimation, one-tap frequency domain equalizer is often used to compensate for received signals distorted by the channel in OFDM systems [13].

$$\hat{X}_k = \frac{Y_k}{\hat{H}_k} \quad (6)$$

where k is the subcarrier index, \hat{X}_k is the equalized signal, \hat{H}_k is the channel estimation in the frequency domain and Y_k is the received signal after the FFT.

$$\hat{H}_k = \frac{Y_{TSk}}{X_{TSk}} \quad (7)$$

After the FFT, channel estimation is calculated using

Eq. 7. Where the transmitted and received training sequences are X_{TSk} and Y_{TSk} , respectively.

Although the one-tap frequency domain equalizer is relatively simple and easy to implement, the significant disadvantage of the method is its susceptibility to noise. Because, if the training symbol is affected by unexpectedly high levels noise, it will introduce bad equalizer coefficients to the receiver.

The suppression of the noise effect is simpler in the time domain than within the frequency domain. Therefore, channel estimation is realized before FFT. Then, $(L-N)$ zeros are added to the end of the channel response array as the length of the channel response (N) is shorter than the number of FFT points (L). Taps on each subcarrier are obtained by the channel response adding zeros, and the FFT operation converting from time domain to frequency domain. The time domain channel estimation to frequency domain channel equalization (TEFE) scheme is shown in Fig. 2.

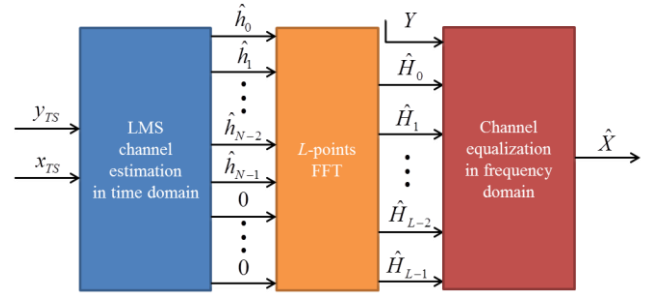


Fig. 2. Time domain channel estimation – frequency domain channel equalization (TEFE) scheme

Recursive least squares (RLS) and least mean square (LMS) are two popular algorithms used in channel estimation within the time domain. RLS-based algorithms have reported good performance levels, but at the costs of increased computational complexity. Since the optical fiber channel changes only very slowly, the LMS algorithm was selected for the proposed method. As shown in Fig. 2, the channel response (\hat{h}_k) is estimated by the LMS algorithm [14]. Then, the channel response (\hat{h}_k) is converted into channel frequency response (\hat{H}_k) by FFT. The equalized signal (\hat{X}) is obtained by using Eq. 6.

4. Channel equalization in time domain

The decision feedback equalizer (DFE) is targeted to recover chosen symbols within the time domain as a cursor symbol, while the inter-symbol interference (ISI) effect of the pre-cursor and post-cursor symbols are canceled by feedforward and feedback filters, respectively [15]. DFE is widely used to compensate for optical channel impairment in coherent optical communication systems [16, 17]. DFE can be considered a nonlinear scheme and can compensate for fiber nonlinearity, but the conventional DFE can only

achieve limited success because feed-forward filter (FFF) and feedback filter (FBF) are linear filters.

The channel-matched filter (CMF)-DFE [15] was selected for channel equalization within the time domain. The block diagram of the CMF-DFE is illustrated in Fig. 3. Using the CMF-DFE, the proposed method increases the optical signal to noise ratio (OSNR) and compensates for fiber nonlinearity and ISI caused by chromatic dispersion within the time domain.

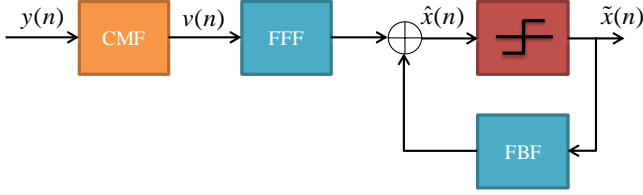


Fig. 3. Block diagram of CMF-DFE

The output of the CMF, $v(n)$, is written as,

$$v(n) = \sum_{k=0}^N \hat{h}_{N-k}^* y(n-k) \quad (8)$$

where \hat{h}_k is the channel response estimated by the LMS algorithm, and $y(n)$ is the channel output. The output of the CMF-DFE equalizer is calculated using,

$$\hat{x}(n) = \sum_{k=-L_{ff}+1}^0 c_k v(n-k) + \sum_{l=1}^{L_{fb}} c_l \tilde{x}(n-l) \quad (9)$$

where c_i 's are equalizer coefficients, $\hat{x}(n)$ and $\tilde{x}(n)$ represents the estimated and detected signals as the output of the CMF-DFE, and L_{ff} and L_{fb} are the number of feed-forward and feedback taps in the DFE, respectively [15].

5. Discrete wavelet transform-based CO-OFDM system

5.1. Discrete wavelet transform basis

The wavelet transform is the representation of a function by an orthogonal set called "wavelets." A Haar wavelet is the simplest type of wavelet. In this paper, Haar wavelet was used as the wavelet function because it reaches the best PAPR performance in [18,19].

Mathematical analysis of the Haar wavelet is given below [19], using,

$$\phi_{01} = \begin{cases} +1 & \text{if } 0 \leq t \leq \frac{1}{2} \\ -1 & \text{if } \frac{1}{2} \leq t \leq 1 \\ 0 & \text{where else} \end{cases} \quad (10)$$

The Haar wavelet family corresponds to the reconstruction low-pass filter h_r and high-pass filter g_r , which are given as the following equations:

$$h_r = \frac{\sqrt{2}}{2} [1, 1] \quad (11)$$

$$g_r = \frac{\sqrt{2}}{2} [1, -1] \quad (12)$$

For the purposes of simplicity, the wavelet family reconstructor has two branches as shown in Fig. 4.

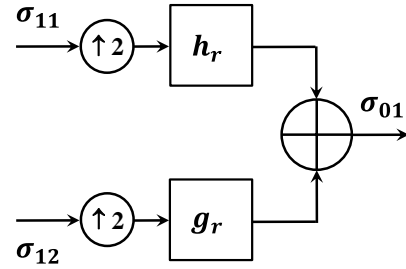


Fig. 4. Two band reconstructor

where σ_{11} and σ_{12} represent the two binary symbols which belong to $\{1, -1\}$. The resulting σ_{01} sequence is described by

$$\sigma_{01}(n) = (\sigma_{11}(\uparrow 2) * h_r)(n) + (\sigma_{12}(\uparrow 2) * g_r)(n) \quad (13)$$

where $*$ shows the convolution product, and $\sigma_{11}(\uparrow 2)$ and $\sigma_{12}(\uparrow 2)$ are the results of dyadic up sampling.

$$\sigma_{11}(n) = \sum_{k=0}^1 h_r(k) \sigma_{11}^{(\uparrow 2)}(n-k) + \sum_{k=0}^1 g_r(k) \sigma_{12}^{(\uparrow 2)}(n-k) \quad (14)$$

Since h_r and g_r are two quadrature mirror filters (QMF) and h_r is symmetric ($h_r(k) = h_r(-k)$), it can be deduced as:

$$\sigma_{11}(n) = \sum_{k=0}^1 h_r(k) \left[\sigma_{11}^{(\uparrow 2)}(n-k) + (-1)^n \sigma_{12}^{(\uparrow 2)}(n-k) \right] \quad (15)$$

It can be also be generalized as the results for the upper bands.

5.2. Proposed CO-OFDM system

Transmitter and receiver blocks within the frequency domain channel equalizer used in the proposed DWT-based CO-OFDM system are shown in Fig. 5.

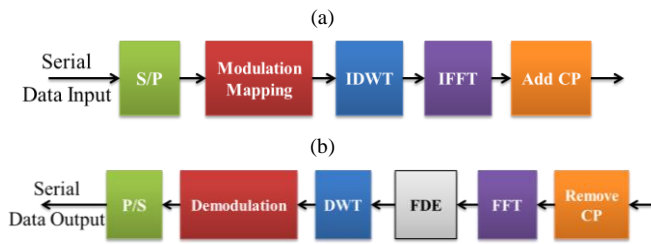


Fig. 5. Block diagram of (a) transmitter and (b) receiver in DWT-based CO-OFDM system

After receiving the serial data from the source, they are paralleled and separated into groups by way of Modulation mapping, based on the number of bits to be transmitted by the subcarriers. OFDM symbols are generated after inverse discrete wavelet transform and inverse fast Fourier transform are taken of the modulated data. The obtained OFDM symbols are passed through the optical channel as shown in Fig. 1. After FFT processing by the receiver, they are equalized by the frequency domain channel equalizer. By applying DWT to the equalized data after demodulation, the data to be sent is decided.

Compared to the conventional CO-OFDM system, the IDWT was added before the IFFT function in the transmitter and DWT was added after the frequency domain equalizer in the receiver of the DWT-based CO-OFDM system. The input data symbols were formed using a DWT matrix as a different subcarrier mapping scheme. This has two advantages. One advantage is that the energy consumption of the input data symbols can be reduced, and that PAPR performance can be increased accordingly. The PAPR for the discrete-time signal $x[n]$ is defined as the ratio of its maximum instantaneous power to its average power and can be expressed as [20],

$$PAPR(x[n]) = \max \frac{|x[n]|^2}{E[x[n]^2]}, 0 \leq n \leq N-1 \quad (16)$$

PAPR performance was evaluated using complementary cumulative distribution function (CCDF). The CCDF curves are shown in Fig. 6 for the conventional CO-OFDM signal and also for the DWT-based CO-OFDM signal in the transmitter. The PAPR performance of the DWT-based CO-OFDM system is seen to outperform the conventional CO-OFDM signal. The second advantage is that the symbols spread to different subcarriers can be collected using DWT in the receiver, and higher BER performance obtained at low OSNR levels.

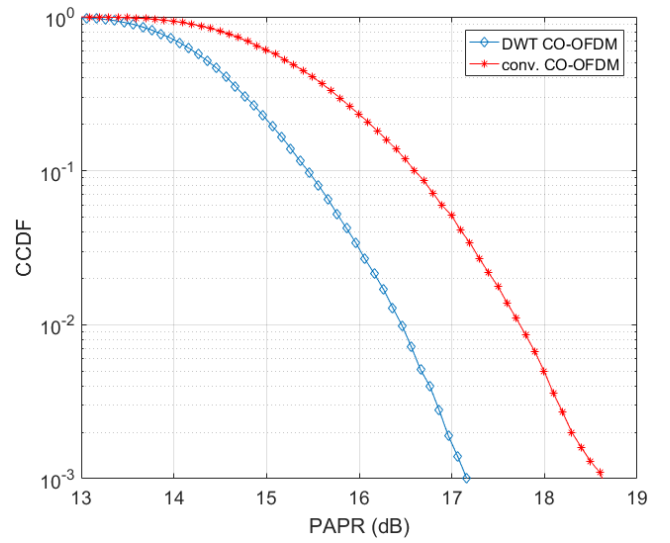


Fig. 6. Comparison of PAPR performances of conventional CO-OFDM and the proposed DWT CO-OFDM for QPSK

Table 1. Fiber optical parameters

Parameter	Value
Wavelength	1550 nm
Velocity of light	200000 km/s
Fiber optical cable length (16QAM,QPSK)	700 – 900 km
Chromatic dispersion parameter	16 ps/(nm.km)
PMD coefficient	0.5 ps/km
Nonlinearity coefficient	1.32 (W.km)^{-1}
Attenuation	0.2 dB/km
Noise figure of EDFA	5 dB
Length of spans	100 km
Fiber	Standard single mode fiber (SSMF)

6. Simulation results

CO-OFDM was designed within a MATLAB-based system, enabling simulation for the transmitter, the receiver and for the channel. Optical signal propagation in

fiber can be modeled by the Non-Linear Schrödinger Equation (NLSE) [21],

$$\frac{\partial A}{\partial z} + \frac{j\beta_2}{2} \frac{\partial^2 A}{\partial t^2} + \frac{\alpha}{2} A = j\gamma A |A|^2 \quad (17)$$

where A is the signal envelope, z is the transmission distance, β_2 is the group velocity dispersion parameter, α is the attenuation coefficient and γ is the nonlinearity factor. The channel block was simulated with the Split-Step Fourier Method (SSFM) for solving NLSE. This system can be made use of by many applications to simulate impairment such as dispersion effects and fiber nonlinearity in optical communication systems [4, 22].

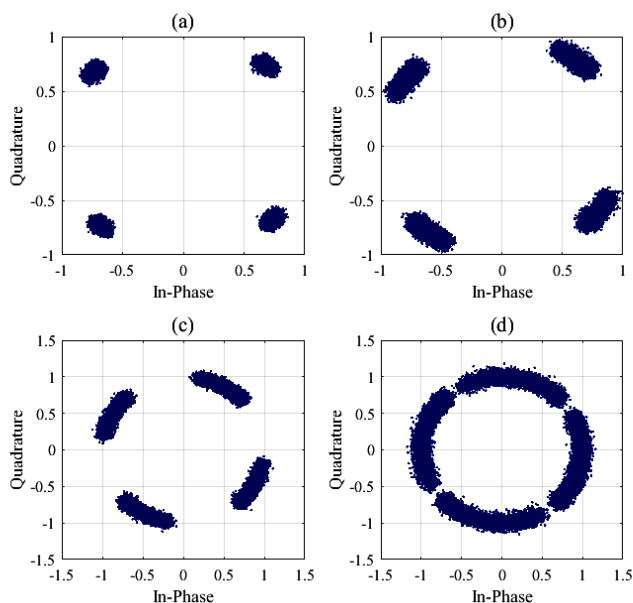


Fig. 7. Output signal constellation of QPSK CO-OFDM systems with Launch power 0 dBm for different transmission length, (a) $L = 100$ km, (b) $L = 300$ km, (c) $L = 600$ km (d) $L = 900$ km

Optical fiber parameters are presented in Table 1. HIPERLAN/2 (IEEE 802.11a) physical layer features were used for OFDM, and simulations were performed over 500 independent channels. In the simulations, the most important parameters of optical communication systems such as fiber nonlinearity, optical noise and dispersion were considered. Dispersion is a linear effect, of which examples are polarization-mode dispersion (PMD) and chromatic dispersion (CD) of optical channels. Fiber nonlinearity only affects the phase of the signals and can cause spectral broadening as shown in Fig. 8. The noise in optical systems is a sum of the electronic thermal noise from the front-end amplifier and shot noise. The noise is modeled as an additive white Gaussian noise. On the transmitter side, the data bits were generated using the Pseudorandom Binary Sequence (PRBS) generator, and then data mapped with the QPSK and 16QAM

modulations. The data transmission bit rates were 10/20 Gbps for QPSK/16QAM modulation.

The signal constellation diagrams of different transmission lengths prior to the channel equalizer are shown in Fig. 7. Due to the CD, which is a function of the transmission length, the constellation points showed a circular and scatter change, and this change increased correspondingly based on the increase in transmission length.

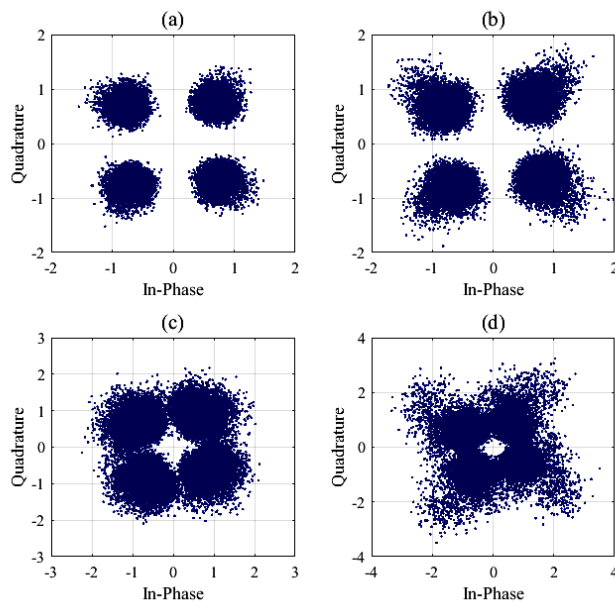


Fig. 8. Output signal constellation of QPSK CO-OFDM systems after 900 km transmission for different launch power, (a) 1 dBm (b) 3 dBm (c) 5 dBm (d) 6 dBm

The constellation diagrams after the channel equalizer at 900 km transmission length and at different launch power values are shown in Fig. 8. Due to high launch power causing greater nonlinear distortion, increased scatter was seen at constellation points as the launch power increased.

The effect of nonlinearity depends on the instantaneous power of the signal according to Non-Linear Schrödinger Equation. Therefore the launch power directly impacts on the system's performance. The signal with the higher power had a greater tolerance for noise, but the higher power can also cause significant nonlinear distortion [16]. Therefore, an optimal launch power level is needed to reach the minimum BER, which varied according to the modulation format.

BER versus launch power performances are shown in Fig. 9 and Fig. 10 for QPSK and 16QAM modulation, respectively. While the BER value decreased at levels lower than the optimal launch power level, the BER value increased at levels higher than the optimal launch power level. For this reason, the fiber cable at low launch power levels was modeled as a linear filter, and the effects of linear impairment and noise were found to be present. However, after the optimal launch power value was

reached, the fiber nonlinearity effect was found to be stronger.

In the equalizers used, the LMS algorithm [14] was used to estimate channel information within the time domain, and the CMF-DFE [13] was used within the time domain equalization process. Also, the intra-symbol frequency domain averaging (ISFA) algorithm was used for the frequency domain equalizer. The ISFA can enhance the frequency response of an optical channel by utilizing training symbols. The ISFA-based frequency domain equalizer is robust against optical channel impairments such as optical noise, CD, PMD, and also fiber nonlinearity [23, 24].

The improved channel coefficient for the subcarrier's k th after the ISFA is calculated using,

$$H(k')_{ISFA} = \frac{1}{\rho} \sum_{k=k'-m}^{k'+m} H(k) \quad (18)$$

$$\rho = \min(k_{\max}, k' + m) - \max(k_{\min}, k' - m)$$

where $H(k)$ is a channel coefficient at the subcarrier's k th. $H(k')_{ISFA}$ is the improved channel coefficient averaged over subcarrier k and its m left neighbors and m right neighbors. k_{\max} and k_{\min} are the maximum and minimum subcarrier indexes, respectively. It is important to select the optimal averaging window size of the ISFA algorithm. Therefore, in this paper, the optimal averaging window sizes (m) of 9 and 5 were chosen for QPSK and 16QAM, respectively.

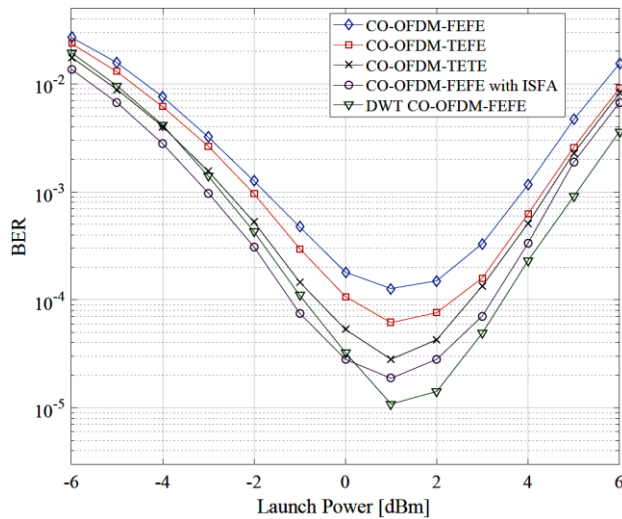


Fig. 9. BER versus launch power for channel equalizers for QPSK modulation after 900 km transmission

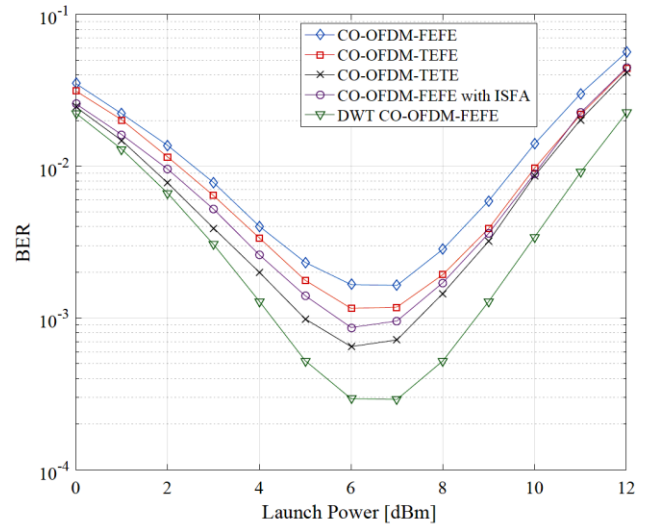


Fig. 10. BER versus launch power for channel equalizers for 16QAM modulation after 700 km transmission

When the performances of CO-OFDM-TETE, CO-OFDM-TEFE, and CO-OFDM-FEFE were compared, CO-OFDM-TETE was found to perform better than both CO-OFDM-TEFE and CO-OFDM-FEFE. A good performance was delivered by CO-OFDM-TETE under low-level launch power when the fiber nonlinearity was not obvious, but its performance was slightly better or similar to that of CO-OFDM-TEFE for QPSK and 16-QAM modulations, respectively, when the launch power was at a higher level.

When the performance of CO-OFDM-FEFE with ISFA was evaluated, as shown in Fig. 9 and Fig. 10, CO-OFDM-FEFE performed better than the methods for QPSK modulation, but the performance of CO-OFDM-FEFE with ISFA in the case of 16QAM modulation was degraded. The reason for this degradation is that the ISFA algorithm reduces the accuracy of channel estimation, because channel frequency responses between adjacent OFDM subcarriers are smoothed in higher-level modulations due to the averaging method.

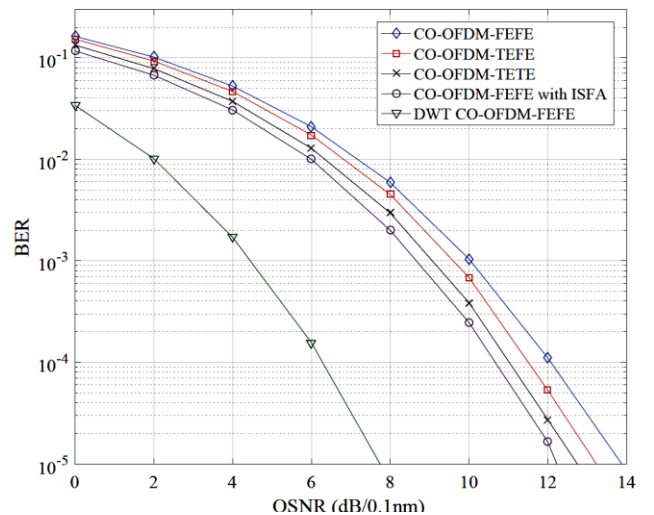


Fig. 11. BER versus OSNR for channel equalizers for QPSK modulation

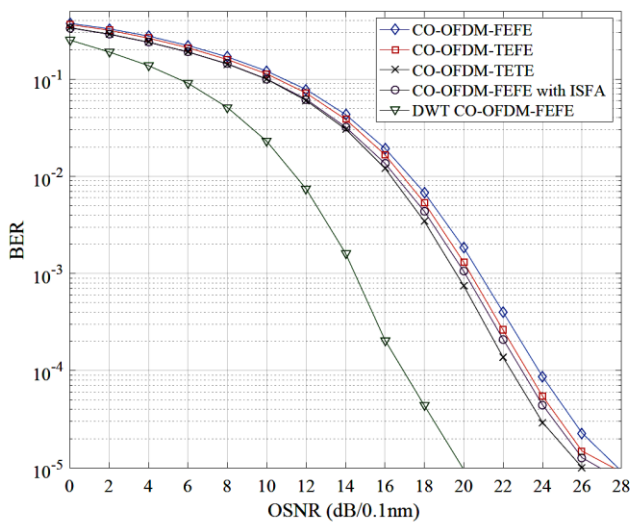


Fig. 12. BER versus OSNR for channel equalizers for 16QAM modulation

At higher levels of fiber nonlinearity, the proposed DWT CO-OFDM-FEFE outperformed the other techniques. The DWT CO-OFDM-FEFE extends the optimal launch power by ~ 1.5 dB compared to the CO-OFDM-TETE in the case of 16QAM modulation for the FEC limit ($BER = 10^{-3}$) value. The reason for this is that DWT spreading can improve the PAPR performance.

In order to analyze the situation where the effect of the fiber nonlinearity is low, BER performances were compared through different optical noise levels at the optimal launch power levels for QPSK and 16-QAM modulated signals. The BER versus optical signal to noise ratio (OSNR) performances of the channel equalizers for QPSK and 16QAM modulation are shown in Fig. 11 and Fig. 12, respectively.

The proposed DWT CO-OFDM-FEFE yields a ~ 5 dB OSNR gain from the nearest equalizer in QPSK modulation for the FEC limit ($BER = 10^{-3}$) value. Similarly, the proposed DWT CO-OFDM-FEFE technique also yields an OSNR gain of ~ 5 dB for 16QAM modulation.

7. Conclusion

Comparative analysis and simulations of BER performances of the conventional CO-OFDM-TETE, CO-OFDM-TEFE, and CO-OFDM-FEFE techniques were performed over optical fiber channels for QPSK and 16-QAM modulations. In the time domain, channel estimation can decrease the effect of optical noise, and CMF-DFE can compensate for linear and nonlinear impairment effects of the optical channel. Therefore, it was shown that BER performances of the conventional CO-OFDM-TETE technique were better than the conventional CO-OFDM-TEFE and CO-OFDM-FEFE techniques.

The aims of the DWT-based CO-OFDM-FEFE system proposed in this paper are that in the transmitter, the PAPR

can be reduced by using IDWT in the conventional CO-OFDM system; and in the receiver, the symbols spread to different subcarriers can be collected through the use of DWT. Therefore, BER performance of the DWT-based CO-OFDM system was improved in regions where fiber nonlinearity was significant and at lower OSNR levels. The obtained performances were achieved from the results of simulations.

It is also noteworthy to state that the proposed method achieved an OSNR gain of approximately 5 dB at the FEC limit ($BER = 10^{-3}$) value for QPSK and 16-QAM modulation. This level of performance achieved with the proposed DWT CO-OFDM-FEFE system is considered to be of value as, in practice it could be easily applied to next-generation 5G, and beyond, wireless communication systems.

References

- [1] Z. Jia, J. Yu, G. K. Chang, *IEEE Photonics Technology Letters* **18**, 1726 (2006).
- [2] G. Charlet, N. Maaref, J. Renaudier, H. Mardoyan, P. Tran, S. Bigo, in *European Conference on Optical Communications 2006*, p. Th.4.3.6.
- [3] A. Lowery, J. Armstrong, in *European Conference and Exhibition on Optical Communication* **2**, 121 (2007).
- [4] A. Yazgan, I. H. Cavdar, *Telecommunication Systems* **55**, 461 (2014).
- [5] M. A. Jarajreh, E. Giacoumidis, I. Aldaya, S. T. Le, A. Tsokanos, Z. Ghassemlooy, N. J. Doran, *IEEE Photonics Technology Letters* **27**, 387 (2015).
- [6] E. Giacoumidis, I. Aldaya, M. A. Jarajreh, A. Tsokanos, S. Le, F. Farjady, Y. Jaouen, A. D. Ellis, N. J. Doran, *IEEE Photonics Technology Letters* **26**, 1383 (2014).
- [7] D. Maiti, M. Brandt-Pearce, *Journal of Lightwave Technology* **33**, 3763 (2015).
- [8] A. Taira, Y. Hara, F. Ishizu, K. Murakami, *Electronics and Communications in Japan (Part I: Communications)* **89**, 10 (2006).
- [9] A. Li, W. Shieh, R. S. Tucker, *Journal of Lightwave Technology* **28**, 3519 (2010).
- [10] Ö. Bulakci, M. Schuster, C. Bunge, B. Spinnler, N. Hanik, in *Conference on Optical Fiber Communication* **1**, 1 (2009).
- [11] H. Zhang, J. Zhang, K. Qiu, *Optik* **125**, 2647 (2014).
- [12] W. Shieh, X. Yi, Y. Ma, Q. Yang, *Journal of Optical Networking* **7**, 234 (2008).
- [13] Y. A. Kao, M. Y. Hsiao, in *Proceedings of Cross Strait Quad-Regional Radio Science and Wireless Technology Conference* **1**, 1615 (2011).
- [14] S. Haykin, *Adaptive filter theory*, 5th Edition (Pearson Publishing, 2014).
- [15] I. Kaya, E. Tugcu, A. Ozen, A. R. Nix, in *IEEE Vehicular Technology Conference* **1**, 1 (2015).
- [16] X. Han, C.-H. Cheng, *Opt. Express* **22**, 8712 (2014).
- [17] P. M. Watts, V. Mikhailov, S. Savory, P. Bayvel, M.

- Glick, M. Lobel, B. Christensen, P. Kirkpatrick, S. S. S. Shang, R. I. Killey, *IEEE Photonics Technology Letters* **17**, 2206 (2005).
- [18] M. Chafii, J. Palicot, R. Gribonval, *Comptes Rendus Physique* **18**, 156 (2017).
- [19] S. Khalid, S. I. Shah, in *International Conference on Emerging Technologies (ICET)* **1**, 179 (2006).
- [20] Y. Wu, C. He, Q. Zhang, Y. Sun, T. Wang, *Optics Express* **26**, 32237 (2018).
- [21] L. Jiang, L. Yan, A. Yi, Y. Pan, W. Pan, B. Luo, *IEEE Photonics Journal* **10**, 1 (2018).
- [22] C. P. Ma, J. W. Kuo, *Japanese Journal of Applied Physics* **43**, 4876 (2004).
- [23] X. Liu, F. Buchali, *Optics Express* **16**, 21944 (2008).
- [24] Q. Yang, N. Kaneda, X. Liu, W. Shieh, *IEEE Photonics Technology Letters* **21**, 1544 (2009).

*Corresponding author: aguner@bingol.edu.tr